

Actin dynamics coupled to clathrin-coated vesicle formation at the trans-Golgi network

Sebastien Carreno,¹ Åsa E. Engqvist-Goldstein,¹ Claire X. Zhang,¹ Kent L. McDonald,² and David G. Drubin¹

¹Department of Molecular and Cell Biology and ²Electron Microscope Laboratory, University of California, Berkeley, Berkeley, CA 94720

In diverse species, actin assembly facilitates clathrin-coated vesicle (CCV) formation during endocytosis. This role might be an adaptation specific to the unique environment at the cell cortex, or it might be fundamental, facilitating CCV formation on different membranes. Proteins of the Sla2p/Hip1R family bind to actin and clathrin at endocytic sites in yeast and mammals. We hypothesized that Hip1R might also coordinate actin assembly with clathrin budding at the trans-Golgi network (TGN). Using deconvolution and time-lapse microscopy, we showed that

Hip1R is present on CCVs emerging from the TGN. These vesicles contain the mannose 6-phosphate receptor involved in targeting proteins to the lysosome, and the actin nucleating Arp2/3 complex. Silencing of Hip1R expression by RNAi resulted in disruption of Golgi organization and accumulation of F-actin structures associated with CCVs on the TGN. Hip1R silencing and actin poisons slowed cathepsin D exit from the TGN. These studies establish roles for Hip1R and actin in CCV budding from the TGN for lysosome biogenesis.

Introduction

In mammalian cells, traffic of newly synthesized hydrolases to the lysosomal compartment is dependent on clathrin and its associated adaptors functioning at the TGN (Campbell and Rome, 1983; Schulze-Lohoff et al., 1985). Recruitment of clathrin triskelia to adaptor complexes at the TGN allows self-assembly of clathrin cages that direct membrane deformation (Brodsky et al., 2001). The cation-dependent mannose 6-P receptor (CD-MPR), which binds to mannose 6-phosphate-modified proteins marked for delivery to lysosomes, is one of several receptors involved in recruitment of the clathrin machinery (Brodsky et al., 2001). The pinching off of clathrin-coated vesicles (CCVs) involves recruitment of the GTPase dynamin, but the fission mechanism and the nature of the force-generating machinery are not known (Jones et al., 1998).

In the recent years, it has been proposed that the actin cytoskeleton plays an important role in endocytosis, another budding event dependent on clathrin and its associated adaptors (Engqvist-Goldstein and Drubin, 2003). Actin may provide forces necessary for vesicle fission and/or propulsion of CCVs away from the plasma membrane. The

involvement of actin in clathrin-mediated endocytosis might be an adaptation specific to the unique environment at the plasma membrane. Alternatively, the role of actin might be fundamental, participating in CCV formation at different membranes.

We have shown that Hip1R and its yeast relative Sla2p, linker proteins that bind to actin, clathrin, and PIP2, are required *in vivo* for functional association between endocytic complexes at the plasma membrane and the actin polymerization machinery (Engqvist-Goldstein et al., 1999, 2001). We proposed that Hip1R and Sla2p may regulate actin polymerization around endocytic buds, promoting the efficient pinching off and/or movement of the plasma membrane-derived vesicles into the cytoplasm (Kaksonen et al., 2003; Engqvist-Goldstein et al., 2004; unpublished data).

Interestingly, it has been reported that short actin filaments are found in close proximity to the Golgi apparatus in mammalian cells, and that some vesicles of Golgi origin are propelled into the cytoplasm by actin polymerization (Frischknecht et al., 1999; Rozelle et al., 2000; Percival et al., 2004). However, it is not clear if or how the actin cytoskeleton plays a role in trafficking events occurring at the TGN.

Since many homologous proteins, including clathrin, adaptor complexes, and dynamin, are present both at endocytic

The online version of this article contains supplemental material.

Address correspondence to David G. Drubin, 16 Barker Hall, Department of Molecular and Cell Biology, University of California, Berkeley, Berkeley, CA 94720-3202. Tel.: (510) 642-3692. Fax: (510) 643-0062. email: drubin@socrates.berkeley.edu

Key words: TGN; lysosomes; clathrin; actin; Hip1R

Abbreviations used in this paper: CCV, clathrin-coated vesicle; CD-MPR, cation-dependent mannose 6-P receptor.

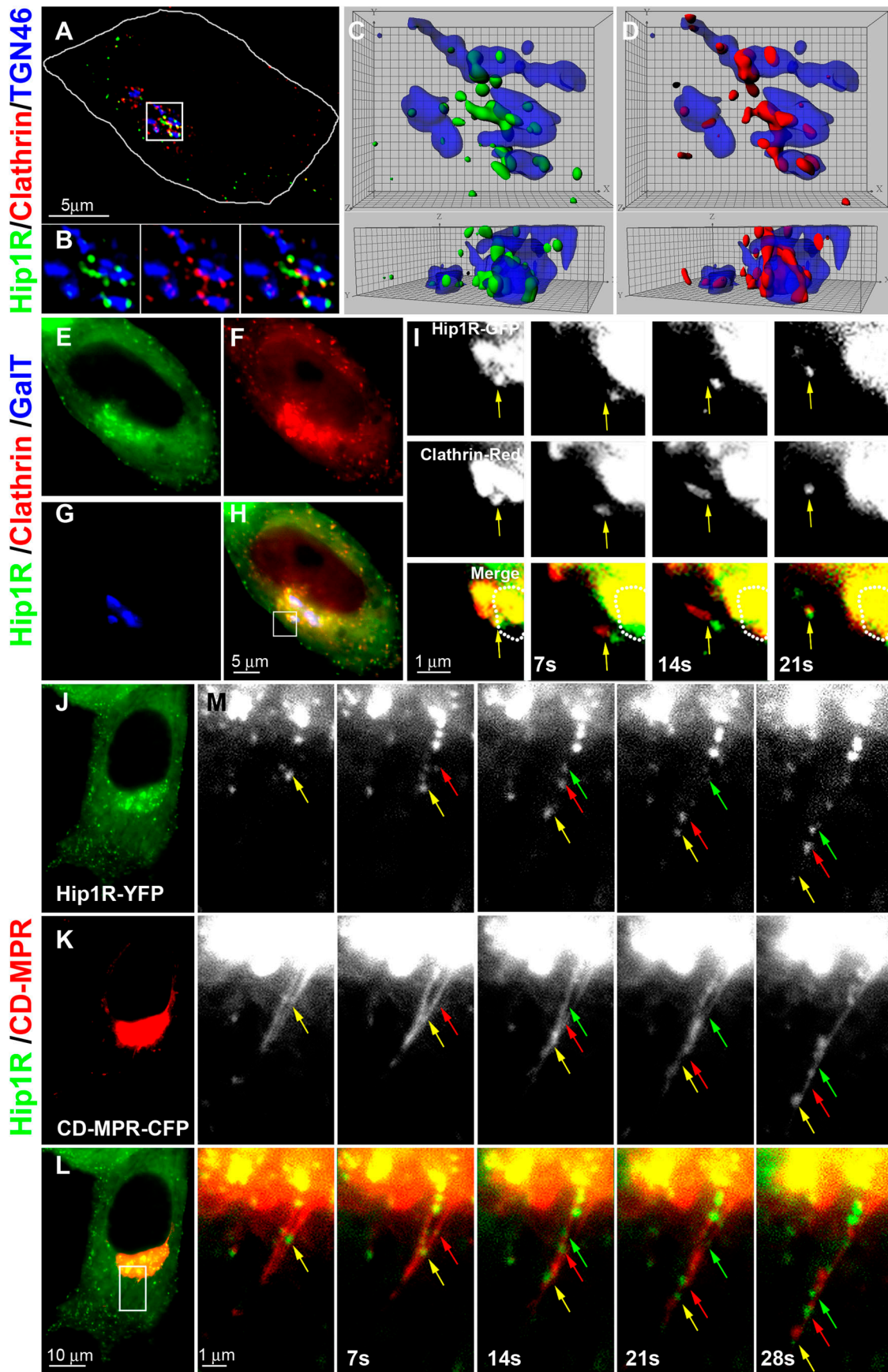


Figure 1. **Fluorescence microscopy analysis of Hip1R intracellular localization.** (A–D) HeLa cells expressing Hip1R-GFP (green) (Engqvist-Goldstein et al., 1999) were fixed and immunostained for clathrin heavy chain (red) and TGN46 (blue). (A and B) Fluorescence data were collected using an API Deltavision DV4 Restoration microscope. Deconvolution was performed using the API SoftWoRx software. (B) Digital

sites and at the TGN, we speculated that the actin cytoskeleton might contribute to clathrin budding at the TGN, as it does at the plasma membrane during endocytosis. We provide evidence that actin and Hip1R participate in trafficking from the TGN to the lysosome.

Results and discussion

We first assessed Hip1R localization in proximity to the TGN in HeLa cells both by immunofluorescence and by expression of a GFP-tagged version of the protein (Engqvist-Goldstein et al., 1999). Using deconvolution microscopy followed by 3D reconstruction, we showed that both endogenous and transfected Hip1R are present on CCVs in close contact with the TGN (Fig. 1, A–D). To analyze the dynamics of TGN-associated Hip1R, we performed time-lapse microscopy on live cells expressing Hip1R-GFP, clathrin-light-chain-DsRed (Gaidarov et al., 1999), and, as a marker of the trans- and medial-Golgi (Llopis et al., 1998), human β 1,4-galactosyltransferase tagged with CFP (GalT-CFP). We observed TGN-derived Hip1R/clathrin vesicles that move away from the TGN (Fig. 1, E–I; see Video 1, available at <http://www.jcb.org/cgi/content/full/jcb.200403120/DC1>). By analyzing Hip1R and CD-MPR dynamics in live cells, we next assessed whether the Hip1R vesicles might be involved in trafficking from the TGN to lysosomes. As described previously, CD-MPR is present on tubular-vesicular structures arising from the TGN (Puertollano et al., 2001). Using the CFP form of the receptor (Barbero et al., 2002), we observed that vesicles containing Hip1R-YFP colocalize with the CD-MPR tubular-vesicular structures (Fig. 1, J–M; see Video 2, available at <http://www.jcb.org/cgi/content/full/jcb.200403120/DC1>).

We previously showed that treatment of HeLa cells with “A2” and “A3” siRNA duplexes directed against two different Hip1R nucleotide sequences leads to a specific 90% and 40–60% decrease, respectively, in Hip1R protein expression (Engqvist-Goldstein et al., 2004). Mock-treated or control siRNA (InvA2)–treated cells showed no reduction. We investigated the distribution and morphology of the TGN in these cells. Immunofluorescence labeling of TGN46 showed that the knock down of Hip1R expression in HeLa cells triggered disruption of the characteristic perinuclear polarized TGN organization (Fig. 2, A–C).

The extent of Hip1R reduction correlated with the level of TGN disruption. Treatment with the A2 or A3 duplex led to dispersion of the TGN in 79% ($n = 418$) or 30% ($n = 282$) of nonmitotic cells, respectively. The TGN ap-

peared dispersed in only 5% ($n = 472$) of the nonmitotic control cells. This TGN dispersion phenotype was not caused by microtubule disruption in Hip1R siRNA–treated cells (unpublished data).

We next used electron microscopy to explore the ultrastructure of the Golgi in cells treated with Hip1R siRNA (Fig. 2, D and E). Whereas the nucleus, endoplasmic reticulum, and mitochondria were normal in A2 cells (unpublished data), the Golgi cisternae appeared swollen with a striking (approximately fivefold) accumulation of buds or vesicles with characteristic clathrin coats (Fig. 2, E and F).

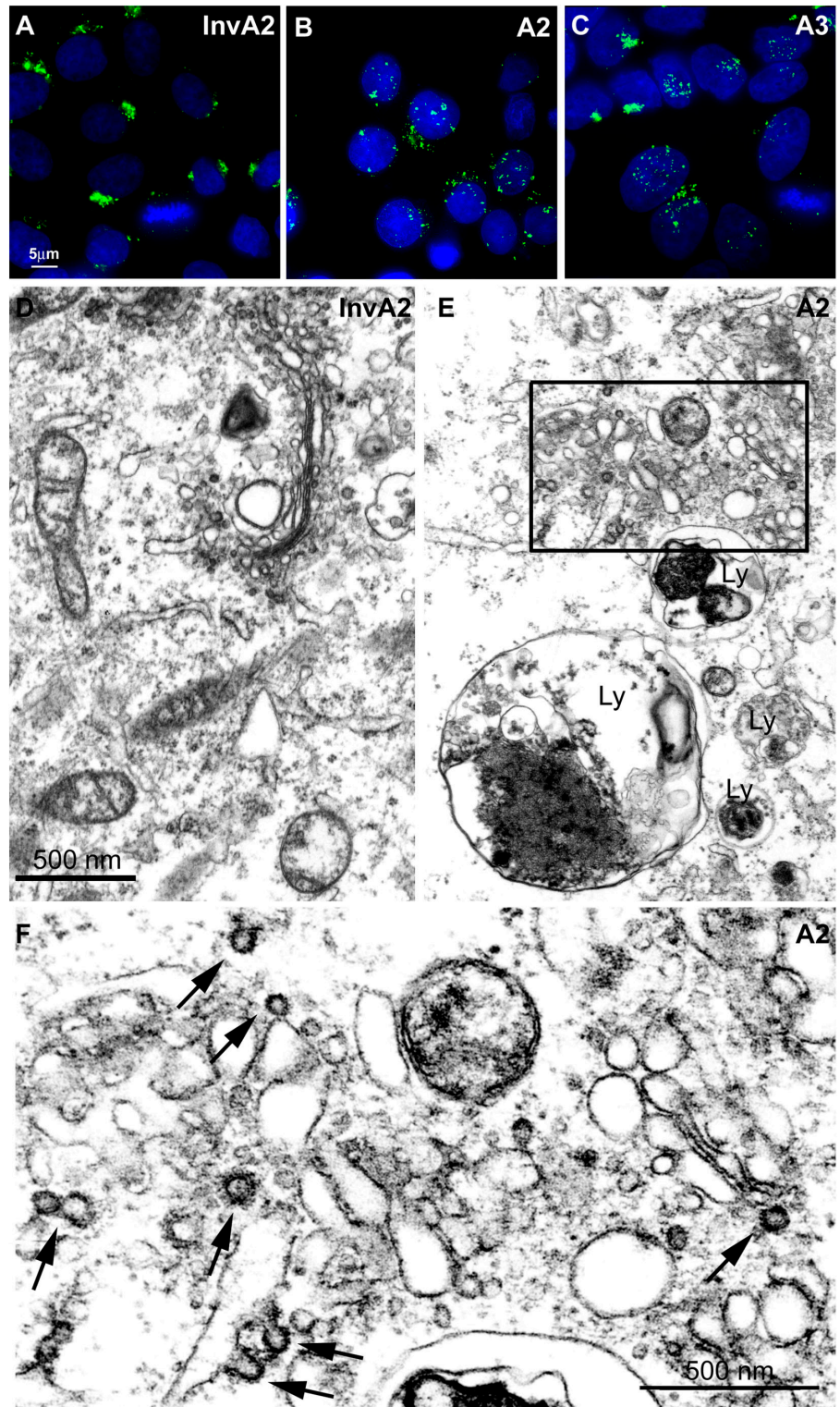
This swelling of the Golgi in cells treated with A2 duplexes could be caused by the impairment of CCV trafficking from the TGN, breaking the balance between inward and outward membrane flux. A similar phenotype was observed in cells knocked down for clathrin light chain expression (Motley et al., 2003). Another characteristic of cells with reduced Hip1R expression levels was an approximately sevenfold increase in the number of structures resembling lysosomes (Fig. 2 E). The accumulation of these structures, which also appeared enlarged relative to similar structures in control cells, could be another consequence of impaired traffic between the TGN and lysosomes, perhaps resulting from impaired lysosome function.

Since depletion of Hip1R or its yeast homologue Sla2 can promote intimate association between actin filaments and endocytic proteins (Kaksonen et al., 2003; Engqvist-Goldstein et al., 2004), we used fluorescent phalloidin to examine actin organization near the TGN in cells treated with Hip1R siRNA duplexes. In control cells, we detected association of actin filaments with TGN membranes using deconvolution microscopy (Fig. 3 A and Table I). However, in cells treated with A2 and A3 siRNA duplexes, there was a seven or threefold increase in the number of these associations, respectively (Fig. 3, B and C, and Table I). Strikingly, the architecture of the actin structures observed in association with the TGN in cells treated with Hip1R siRNA duplexes was very distinct from that observed in control cells. In cells depleted for Hip1R, the actin structures were substantially bigger, and they appeared as curved tails or rings (Fig. 3, A–C, inset), similar to the structures seen at endocytic sites in cells compromised for Hip1R or Sla2p expression (Kaksonen et al., 2003; Engqvist-Goldstein et al., 2004).

The association of actin with the TGN seen at low frequency in control cells could reflect a transient association during the dynamic process of CCV formation. This association may become deregulated in cells treated with the A2 and A3 duplexes. Perhaps Hip1R negatively regulates actin

magnification of the TGN area boxed in A. (C and D) Three-dimensional volume (Top, top view; Bottom, side view) rendering of the area shown in B, made using 15 successive deconvolved planes using Imaris4.0 (Bitplane). (C) TGN46 (blue) and Hip1R (green). (D) TGN46 (blue) and clathrin (red). (E–H) Time-lapse microscopy imaging of live HeLa cells expressing (E) Hip1R-GFP (Engqvist-Goldstein et al., 1999), (F) dsRed-clathrin LC isoform a (LCA) (Gaidarov et al., 1999), (G) GalT-CFP (CLONTECH Laboratories, Inc.) as a TGN marker. (H) Merged image. (I) Magnification of the region boxed in H. Images were acquired using an API Deltavision DV4 microscope at the intervals indicated. The white dashed line in the merged image represents the edge of the GalT-CFP signal at the beginning of the time-lapse experiment. Arrows track individual Hip1R/clathrin vesicle arising from the TGN. The shift between Hip1R-GFP and dsRed-clathrin in I is due to the time delay for image acquisition between the two fluorescence channels (see Video 1, available at <http://www.jcb.org/cgi/content/full/jcb.200403120/DC1>). (J–M) Time-lapse microscopy imaging of HeLa cells expressing (J) Hip1R-YFP or (K) CD-MPR-CFP (Barbero et al., 2002). (L) Merged image. (M) Magnification of the region boxed in L. Images were acquired using an API Deltavision DV4 microscope at the indicated intervals. Arrows track individual Hip1R vesicles aligned along tubulo-vesicular structures emerging from the TGN (see Video 2, available at <http://www.jcb.org/cgi/content/full/jcb.200403120/DC1>).

Figure 2. Effect of Hip1R knock down on TGN morphology of HeLa cells. (A–C) HeLa cells treated with the indicated siRNA duplexes for 3 d were fixed, and then TGN46 (green) and nuclei (DAPI, blue) were labeled with antibodies and dye, respectively. Cells were imaged using an inverted Nikon Eclipse TE300 fluorescence microscope (Nikon) with a Nikon Plan Apo (1.4NA) 100× objective and a Hamamatsu ORCA cooled CCD camera (Hamamatsu). (D–F) Electron micrographs of HeLa cells treated with the InvA2 siRNA (D) and A2 siRNA (E). Cells depleted for Hip1R show an accumulation of lysosome (Ly) and of clathrin-coated buds or vesicles. (F) Magnification of the region boxed in E. Arrows, clathrin-coated buds or vesicles.



polymerization during CCV formation so that polymerization only occurs at the appropriate moment when it can promote vesicle release.

We next investigated whether the TGN-associated actin filaments are present at areas of the organelle that are specialized for sorting to lysosomes. In control cells, F-actin was detected in association with ~5% of the CCVs on TGN membranes, and CCVs were detected in association with

about one third of the F-actin structures on TGN membranes (Fig. 3 D and Table I), consistent with a transient role for actin in the CCV formation. Hip1R depletion by A2 siRNA treatment led to a sixfold increase in the association of F-actin with CCVs on the TGN, and to a twofold increase in the proportion of TGN-associated actin structures that localized with CCVs, supporting the hypothesis that Hip1R negatively regulates actin assembly during CCV

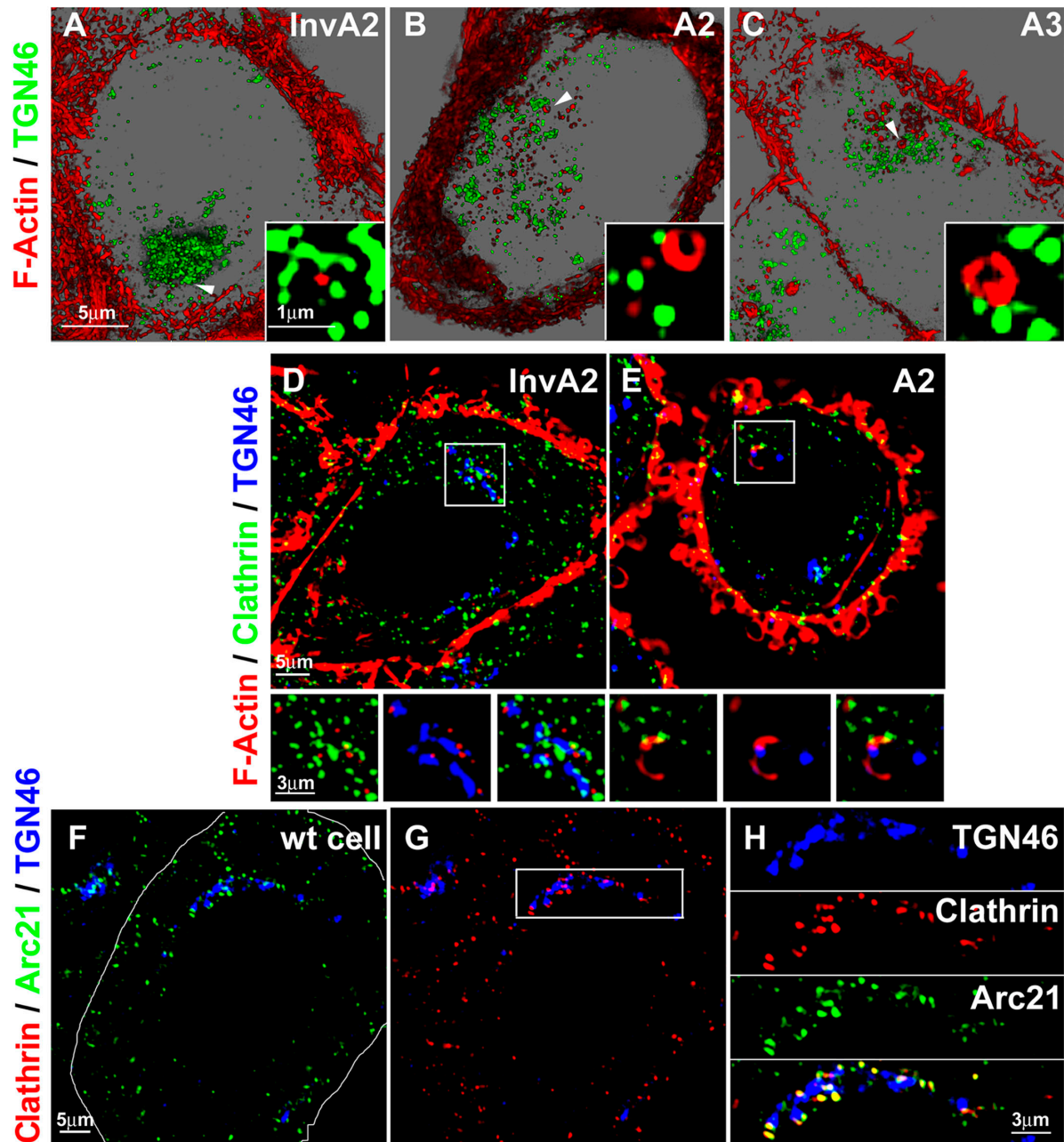


Figure 3. Interaction between actin filaments and clathrin structures at the TGN of control and Hip1R knock down cells. (A–C) Association of F-actin structures with TGN membranes. HeLa cells treated for 3 d with the indicated siRNA duplexes were fixed and labeled for filamentous actin (red) and for TGN46 (green). Fluorescence data were collected and deconvolved as described in Fig. 1. Pictures were generated using 30 deconvolved planes with the blend section mode of Imaris3.2 (Bitplane) and represent a 3D projection of a 3- μ m optical section. Inset, magnifications of deconvolved regions (white arrow on A–C) showing typical F-actin/TGN structures. (D and E) F-actin is associated with clathrin at the TGN. HeLa cells treated for 3 d with the indicated siRNA duplexes were fixed and stained for clathrin heavy chain (green), TGN46 (blue), and F-actin (red). Fluorescence data were collected and deconvolved as described in Fig. 1. Bottom panels, magnifications of boxed region. (F–H) Association of the Arp2/3 complex with clathrin-coated buds/vesicles at the TGN in untreated HeLa cells. HeLa cells were fixed and stained for clathrin heavy chain (red), TGN46 (blue), and the Arp2/3 complex (green) (detected using a p21-Arc:FITC antibody). (H) Digital magnification of the boxed region.

formation at the TGN, and that its depletion stabilizes the association between CCVs on the TGN and F-actin (Fig. 3 E and Table I). This observation suggests that actin regulation by Hip1R is necessary for the efficient release of CCVs from the TGN. Another possibility, however, is that this actin regulation is necessary for subsequent movements of the clathrin vesicle after its release.

The Arp2/3 complex, which promotes actin assembly by nucleating actin filaments, has been localized in the perinuclear region (Welch et al., 1997). However, this localization has never been analyzed in detail. Using deconvolution microscopy, we showed that the Arp2/3 complex (revealed by an antibody directed against its Arc21 subunit) is localized on TGN-derived CCVs. (Fig. 3, F and G). Together, these

Table I. Comparison of F-actin structures associated with the TGN in control and Hip1R siRNA cells

	InvA2	A2	A3
Number of actin structures in association with the TGN	9.6 ± 3.5	66 ± 18.4	32.3 ± 5.9
F-actin structures in association with clathrin on the TGN/ total F-actin structures in the TGN area	38.9%	72.4%	ND
Clathrin structures on the TGN associated with F-actin structures/ total clathrin structures on the TGN	5.3%	34.3%	ND

Cells were labeled for F-actin and immunostained for clathrin and TGN46 as described in the Materials and methods. Fluorescence data for the entire cell were collected using an API Deltavision DV4 Restoration microscope, with an increment in the Z axis of 100 nm. Deconvolution was carried out using the API SoftWoRx software. The number of F-actin structures and clathrin structures in association with TGN46 was then manually determined using the blend section mode of Imaris3.2 (Bitplane) with a Z projection of 1 mm in order to identify 3D structures.

data provide evidence for a role for actin dynamics in the clathrin-dependent exit from the TGN. We propose that actin assembly on the TGN is tightly controlled. The Arp2/3 complex stimulates assembly, while Hip1R limits assembly.

To test the biological importance of our hypothesis that actin assembly under regulation by Hip1R participates in trafficking from the TGN to lysosomes, we monitored the maturation of the lysosomal hydrolase cathepsin D in cells treated with the A2 and InvA2 duplexes, or treated with an actin poison. The exit of this hydrolase from the TGN is mainly dependent on the clathrin machinery (Godbold et al., 1998). Cathepsin D is present in the TGN as a pro-enzyme, pro-cathepsin D, which gets processed to an active form when it reaches endosomes. This mature form is eventually cleaved into heavy and light chains when it reaches lysosomes. A2 siRNA treatment inhibited the exit of pro-cathepsin D from the Golgi apparatus (Fig. 4 A). At the end of a 4-h chase, 56.8% (±6.8%) of the cathepsin D was still in its pro-enzyme form, suggesting that it is retained in the Golgi of Hip1R-depleted cells. In comparison, in control cells only 21.4% (±3%) of the hydrolase was in its pro-enzyme form after a 4-h chase. To confirm that this effect was a specific result of the Hip1R knock down, we constructed a cell line that expresses a Hip1R cDNA that is not targeted by the A2 siRNA. When this cell line was treated with the A2 siRNA duplex, expression of Hip1R carrying the silent mutation was sufficient to restore the cathepsin D maturation rate to levels seen in the same cell line treated with the InvA2 siRNA duplex (Fig. 4 B), and to prevent TGN dispersion (unpublished data).

Depending on the cell type, a variable fraction of cathepsin D escapes MPR sorting in the TGN and is instead mistargeted to the plasma membrane independent of the clathrin-mediated route (Godbold et al., 1998). In cells expressing various inactive mutants of the CD-MPR, cathepsin D is mostly secreted because the mannose 6-phosphate-modified hydrolases are not sorted to the TGN-clathrin route (Munier-Lehmann et al., 1996). We therefore collected the media in which cells treated with the A2 or InvA2 duplexes had been grown and performed cathepsin D immunoprecipitations. We did not observe any difference in the efficiency of cathepsin D secretion (Fig. 4 C). The fraction of cathepsin D present in the media after a 4-h chase was 40% of the total cathepsin D under both conditions. These data indicate that cathepsin D secretion is not impaired in cells deficient in Hip1R expression. They also suggest that when Hip1R is depleted, cathepsin D might remain trapped by the CD-MPR in the area of the TGN

dedicated to sorting to lysosomes. Otherwise, higher levels of cathepsin D secretion might have been observed.

We next tested the importance of actin for trafficking from the TGN to lysosomes. We immunoprecipitated cathepsin D from cells treated during the chase of a pulse-chase experi-

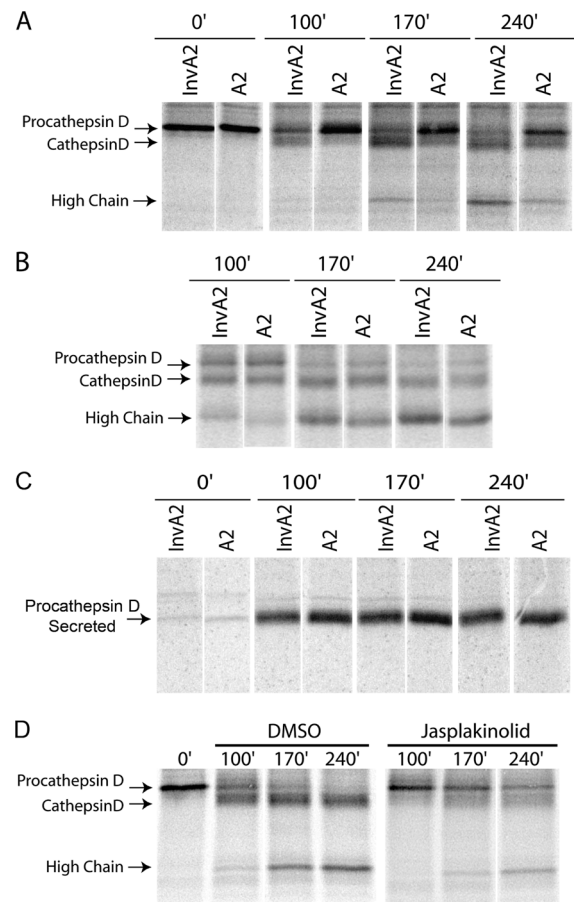


Figure 4. Effect of Hip1R depletion or Jasplakinolide treatment on cathepsin D maturation. (A and B) Wild-type HeLa cells or (B) HeLa cells stably expressing a Hip1R "rescue" cDNA were treated with A2 or InvA2 siRNA duplexes for 3 d before the pulse-chase experiment. At the indicated chase times, the cells were lysed and intracellular cathepsin D was immunoprecipitated from the lysate. (C) The secreted cathepsin D from cells in A was immunoprecipitated from the medium. (D) Wild-type HeLa cells were treated with DMSO or 10 μ g/ml Jasplakinolide during the chase. At the indicated chase times, the cells were lysed, and intracellular cathepsin D was immunoprecipitated from the lysate. White lines indicate that intervening lanes have been spliced out.

ment with the actin poison Jasplakinolide, or with its carrier, DMSO. Jasplakinolide had a severe effect on cathepsin D maturation, with 39% ($\pm 2\%$) of the cathepsin D retained in the Golgi after a 4-h chase. By this time, cathepsin D had completely exited from the Golgi of control cells (Fig. 4 D). Two other actin poisons, cytochalasin D and latrunculin A, both caused a similar defect in cathepsin D maturation (unpublished data), confirming that actin dynamics are important for trafficking from the TGN to lysosomes.

We have established a novel role for actin dynamics in trafficking from the TGN to lysosomes and have demonstrated that Hip1R is necessary for productive coupling of actin dynamics to this pathway. The importance of actin dynamics, proteins of the Hip1R/Sla2p family, and the Arp2/3 complex were established previously for endocytosis in yeast and mammalian cells (Merrifield et al., 2002; Kaksonen et al., 2003; Engqvist-Goldstein et al., 2004). We propose that in addition to an endocytic role that is conserved across species, these proteins also function at the specialized area of the TGN from which CCVs bud for trafficking to lysosomes.

Materials and methods

siRNA preparation and treatment of HeLa cells with siRNA

For details of siRNA sequences, preparation, and use see (Engqvist-Goldstein et al., 2004).

DNA constructs

The wild-type human Hip1R cDNA was a gift from T. Suzuki (Shinshu University School of Medicine, Matsumoto, Japan) (Okano et al., 2003). hsHip1R was amplified by PCR using primers that generate ClaI and NheI sites at the 5' and 3' ends, respectively. The PCR products were ligated into pIRES-Neo2 (CLONTECH Laboratories, Inc.). Several silent mutations were generated in these constructs (C2478G, C2481T, and A2484C) in the region targeted by siRNA-A2 (nucleotide 2473–2493). These were created to prevent siRNA-A2 from targeting mRNA derived from the stably expressed exogenous Hip1R. Constructions of Hip1R-GFP and Hip1R-YFP were described previously (Engqvist-Goldstein et al., 1999, 2001).

The cDNA encoding CD-MPR-CFP was a gift from S. Pfeffer (Stanford University School of Medicine, Stanford, CA) (Barbero et al., 2002). The trans-Golgi marker pECFP-Golgi, encoding CFP fused to the NH₂-terminal region of human β 1,4-galactosyltransferase, was purchased from CLONTECH Laboratories, Inc.

Cell culture and indirect immunofluorescence

Cell culture and immunofluorescence were performed as described previously (Engqvist-Goldstein et al., 1999). HeLa cells were grown in DME containing 10% FBS. For immunofluorescence analysis, cells were transfected with siRNA on glass coverslips in 24-well plates for 3 d. The following primary antibodies were used: anti-Hip1R antibody (Rb#2855) was used at 1:50; anti-clathrin antibody (X22) (Affinity BioReagents, Inc.) was used at 1:500; anti-human TGN46 antibody (Serotek) was used at 1:1,000; anti-p21-Arc:FITC antibody (BD Transduction Laboratories) was used at 1:25. FITC-conjugated donkey anti-rabbit, FITC- or TRITC-conjugated donkey anti-mouse IgGs, and Cy5-conjugated donkey anti-sheep were purchased from Jackson ImmunoResearch Laboratories and used according to the manufacturer's directions. Texas red-X phalloidin (Molecular Probes) was used at 1:500 for F-actin staining.

Deconvolution microscopy and 3D reconstruction

Fluorescence data were collected using an API Deltavision DV4 Restoration microscope. Voxels were collected at 67-nm lateral and 100-nm axial intervals. Deconvolution was performed using the API SoftWoRx software on a Linux 2.8GHz workstation. Rendering of the 3D data was performed using Imaris3.2 (Bitplane) on a Windows XP 2.8GHz workstation.

Time-lapse microscopy

HeLa cells grown on 20-mm glass coverslips were observed 16–20 h after fuge 6 transfection (Roche Diagnostics). The coverslips were mounted

on a temperature-controlled stage. During observation, cells were maintained in F-12 media (Invitrogen) containing 5% fetal calf serum and 10 mM Hepes, pH 7.4. Cells coexpressing low levels of the XFP constructs were imaged using an API Deltavision DV4 Restoration microscope at the intervals indicated. XFP fluorescence was visualized with 400–1,000-ms exposures. For time-lapse acquisition of dsRed-clathrin LC, Hip1R-GFP, and GalT-CFP, a time-lapse dsRed/GFP movie was acquired, enclosed between two single time point acquisitions in the CFP canal.

Rescue experiments

Stable cell lines expressing human Hip1R were generated using standard procedures. A stable cell line expressing the vector alone was also generated as a control. For rescue experiments, these stable cell lines expressing Hip1R were treated with siRNA (invA2, A2) as described above.

Cathepsin D maturation

Pulse-chase metabolic labeling and cathepsin D immunoprecipitations were performed on adherent HeLa cells plated on 6-well plates as described previously with 10 mM mannose 6-P in the media to block enzyme recapture (Stinchcombe et al., 2000). A rabbit anti-human cathepsin D antiserum (DAKO Corporation) was used for immunoprecipitations.

Electron microscopy

Cells were grown on Aclar plastic and then fixed as previously published (McDonald, 1984). After polymerization of the resin, the Aclar was peeled away, and cells were remounted for sectioning. Sections 60 nm thick were cut on a Leica Ultracut E microtome, post-stained with uranyl acetate and lead citrate, and viewed in an FEI 12 electron microscope operating at 100 kV.

Online supplemental material

Two supplemental videos are available online at <http://www.jcb.org/cgi/content/full/jcb.200403120/DC1>. Video 1 corresponds to Fig. 1 I and shows Hip1R-GFP (green) and clathrin-dsRed (red) in HeLa cells 24 h after transfection. Video 2 corresponds to Fig. 1 M and shows Hip1R-YFP (green) and CD-MPR-CFP (red) in HeLa cells 24 h after transfection.

The deconvolution microscopy was done in the CNR Biological Imaging facility at University of California, Berkeley. We thank Steve Ruzin and Denise Schichnes for their advice on deconvolution microscopy and image restoration and Ann Fischer for her advice on cell culture. We also thank Suzanne Pfeffer, Randy Schekman, Stuart Kornfeld, and Ann Erickson for advice and reagents.

This work was supported by National Institutes of Health grant GM65462 to D.G. Drubin. S. Carreno was supported by the Human Frontier Science Program.

Submitted: 22 March 2004

Accepted: 4 May 2004

References

- Barbero, P., L. Bittova, and S.R. Pfeffer. 2002. Visualization of Rab9-mediated vesicle transport from endosomes to the trans-Golgi in living cells. *J. Cell Biol.* 156:511–518.
- Brodsky, F.M., C.Y. Chen, C. Kneuhl, M.C. Towler, and D.E. Wakeham. 2001. Biological basket weaving: formation and function of clathrin-coated vesicles. *Annu. Rev. Cell Dev. Biol.* 17:517–568.
- Campbell, C.H., and L.H. Rome. 1983. Coated vesicles from rat liver and calf brain contain lysosomal enzymes bound to mannose 6-phosphate receptors. *J. Biol. Chem.* 258:13347–13352.
- Engqvist-Goldstein, A.E., and D.G. Drubin. 2003. Actin assembly and endocytosis: from yeast to mammals. *Annu. Rev. Cell Dev. Biol.* 19:287–332.
- Engqvist-Goldstein, A.E., M.M. Kessels, V.S. Chopra, M.R. Hayden, and D.G. Drubin. 1999. An actin-binding protein of the Sla2/Huntingtin interacting protein 1 family is a novel component of clathrin-coated pits and vesicles. *J. Cell Biol.* 147:1503–1518.
- Engqvist-Goldstein, A.E., R.A. Warren, M.M. Kessels, J.H. Keen, J. Heuser, and D.G. Drubin. 2001. The actin-binding protein Hip1R associates with clathrin during early stages of endocytosis and promotes clathrin assembly in vitro. *J. Cell Biol.* 154:1209–1223.
- Engqvist-Goldstein, A.E., C.X. Zhang, S. Carreno, C. Barroso, J. Heuser, and D.G. Drubin. 2004. RNAi-mediated Hip1R silencing results in stable asso-

- ciation between the endocytic machinery and the actin assembly machinery. *Mol. Biol. Cell.* 15:1666–1679.
- Frischknecht, F., S. Cudmore, V. Moreau, I. Reckmann, S. Rottger, and M. Way. 1999. Tyrosine phosphorylation is required for actin-based motility of *Vaccinia* but not *Listeria* or *Shigella*. *Curr. Biol.* 9:89–92.
- Gaidarov, I., F. Santini, R.A. Warren, and J.H. Keen. 1999. Spatial control of coated-pit dynamics in living cells. *Nat. Cell Biol.* 1:1–7.
- Godbold, G.D., K. Ahn, S. Yeyeodu, L.F. Lee, J.P. Ting, and A.H. Erickson. 1998. Biosynthesis and intracellular targeting of the lysosomal aspartic proteinase cathepsin D. *Adv. Exp. Med. Biol.* 436:153–162.
- Jones, S.M., K.E. Howell, J.R. Henley, H. Cao, and M.A. McNiven. 1998. Role of dynamin in the formation of transport vesicles from the trans-Golgi network. *Science.* 279:573–577.
- Kaksonen, M., Y. Sun, and D.G. Drubin. 2003. A pathway for association of receptors, adaptors, and actin during endocytic internalization. *Cell.* 115:475–487.
- Llopis, J., J.M. McCaffery, A. Miyawaki, M.G. Farquhar, and R.Y. Tsien. 1998. Measurement of cytosolic, mitochondrial, and Golgi pH in single living cells with green fluorescent proteins. *Proc. Natl. Acad. Sci. USA.* 95:6803–6808.
- McDonald, K. 1984. Osmium ferricyanide fixation improves microfilament preservation and membrane visualization in a variety of animal cell types. *J. Ultrastruct. Res.* 86:107–118.
- Merrifield, C.J., M.E. Feldman, L. Wan, and W. Almers. 2002. Imaging actin and dynamin recruitment during invagination of single clathrin-coated pits. *Nat. Cell Biol.* 4:691–698.
- Motley, A., N.A. Bright, M.N. Seaman, and M.S. Robinson. 2003. Clathrin-mediated endocytosis in AP-2-depleted cells. *J. Cell Biol.* 162:909–918.
- Munier-Lehmann, H., F. Mauxion, U. Bauer, P. Lobel, and B. Hoflack. 1996. Re-expression of the mannose 6-phosphate receptors in receptor-deficient fibroblasts. Complementary function of the two mannose 6-phosphate receptors in lysosomal enzyme targeting. *J. Biol. Chem.* 271:15166–15174.
- Okano, A., N. Usuda, K. Furihata, K. Nakayama, Q. Bao Tian, T. Okamoto, and T. Suzuki. 2003. Huntingtin-interacting protein-1-related protein of rat (rHIP1R) is localized in the postsynaptic regions. *Brain Res.* 967:210–225.
- Percival, J.M., J.A. Hughes, D.L. Brown, G. Schevzov, K. Heimann, B. Vrhovski, N. Bryce, J.L. Stow, and P.W. Gunning. 2004. Targeting of a tropomyosin isoform to short microfilaments associated with the Golgi complex. *Mol. Biol. Cell.* 15:268–290.
- Puertollano, R., R.C. Aguilar, I. Gorshkova, R.J. Crouch, and J.S. Bonifacino. 2001. Sorting of mannose 6-phosphate receptors mediated by the GGAs. *Science.* 292:1712–1716.
- Rozelle, A.L., L.M. Machesky, M. Yamamoto, M.H. Driessens, R.H. Insall, M.G. Roth, K. Luby-Phelps, G. Marriott, A. Hall, and H.L. Yin. 2000. Phosphatidylinositol 4,5-bisphosphate induces actin-based movement of raft-enriched vesicles through WASP-Arp2/3. *Curr. Biol.* 10:311–320.
- Schulze-Lohoff, E., A. Hasilik, and K. von Figura. 1985. Cathepsin D precursors in clathrin-coated organelles from human fibroblasts. *J. Cell Biol.* 101:824–829.
- Stinchcombe, J.C., L.J. Page, and G.M. Griffiths. 2000. Secretory lysosome biogenesis in cytotoxic T lymphocytes from normal and Chediak Higashi syndrome patients. *Traffic.* 1:435–444.
- Welch, M.D., A.H. DePace, S. Verma, A. Iwamatsu, and T.J. Mitchison. 1997. The human Arp2/3 complex is composed of evolutionarily conserved subunits and is localized to cellular regions of dynamic actin filament assembly. *J. Cell Biol.* 138:375–384.